HHS Public Access

Author manuscript

Adv Mater. Author manuscript; available in PMC 2022 August 01.

Published in final edited form as:

Adv Mater. 2021 August ; 33(32): e2008809. doi:10.1002/adma.202008809.

Reversible Photothermal Modulation of Electrical Activity of Excitable Cells using Polydopamine Nanoparticles

Hamed Gholami Derami, **Prashant Gupta**

Department of Mechanical Engineering and Materials Science, Institute of Materials Science and Engineering, Washington University in St. Louis, St. Louis, MO 63130, USA

Kuo-Chan Weng

Department of Biomedical Engineering, Washington University in St. Louis, St. Louis, MO 63130, USA

Anushree Seth, **Rohit Gupta**

Department of Mechanical Engineering and Materials Science, Institute of Materials Science and Engineering, Washington University in St. Louis, St. Louis, MO 63130, USA

Jonathan R. Silva, **Baranidharan Raman**

Department of Biomedical Engineering, Washington University in St. Louis, St. Louis, MO 63130, USA

Srikanth Singamaneni

Department of Mechanical Engineering and Materials Science, Institute of Materials Science and Engineering, Washington University in St. Louis, St. Louis, MO 63130, USA

Abstract

Advances in the design and synthesis of nanomaterials with desired biophysicochemical properties can be harnessed to develop non-invasive neuromodulation technologies. Here, we demonstrate the reversible modulation of the electrical activity of neurons and cardiomyocytes using polydopamine (PDA) nanoparticles as photothermal nanotransducers. In addition to their broad light absorption and excellent photothermal activity, PDA nanoparticles are highly biocompatible and biodegradable, making them excellent candidates for both *in vitro* and *in vivo* applications. The modulation of the activity (*i.e.* spike rate of the neurons and beating rate of cardiomyocytes) of excitable cells could be finely controlled by varying the excitation power density and irradiation duration. Under optimal conditions, we demonstrate reversible suppression (~100%) of neural activity and reversible enhancement (two-fold) in the beating rate of cardiomyocytes. To improve the ease of interfacing of photothermal transducers with these excitable cells and enable spatial localization of the photothermal stimulus, we have realized a collagen/PDA nanoparticle foam, which can be used as an “add-on patch” for photothermal stimulation. The non-genetic optical neuromodulation approach using biocompatible and biodegradable nanoparticles represents a

barani@wustl.edu, singamaneni@wustl.edu.

Supporting Information

Supporting Information is available from the Wiley Online Library or from the author.

minimally-invasive method for controlling the activity of excitable cells with potential applications in nano-neuroscience and engineering.

Graphical Abstract

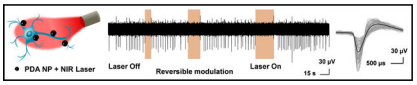

Keywords

neuromodulation; photothermal stimulation; polydopamine nanoparticles; light-to-heat conversion; nano-neuro interface

Introduction

Controlling a selective population of neurons to understand and establish a causal link between the neural activity and overall behavioral outcomes is a grand challenge in systems neuroscience. Harnessing the unique properties of matter at the nanoscale to tackle this grand challenge has received increased attention over the past few years.[1] Among the many methods that aim to modulate the biological processes, a particularly attractive method is photo-regulation, a process in which light is utilized as an external stimulus [2]. Since cells by themselves are not sensitive to photo-stimulation, insertion of light-sensitive ion channels and subsequent stimulation of these neurons for selective control (i.e. optogenetics), has become an increasingly popular and staple tool for numerous investigations.[3] While optogenetic techniques are promising and have revolutionized basic research aimed at understanding the computational and behavioral role of several different neural populations, there are still several limitations associated with these techniques that remain to be addressed.[4] These include: (i) ability to excite neurons that are embedded deep in the tissue; (ii) ability to be widely used in different model organisms with or without a rich repertoire of genetic tools; (iii) graded control of neurons; (iv) ability to control different subset of neurons in a concurrent fashion; (v) reversibility of the proposed approaches to return the controlled neurons to their original configuration; and more importantly (vi) feasibility of developing a non-invasive approach. To address some of these shortcomings, the use of nanomaterials for non-genetic electrical and thermal stimulation were explored and tested successfully in recent years.[5] Among these, photothermal methods have shown great promise and versatility in stimulating neuronal cells [6].

It has been reported that the absorption of the infrared (IR) light by water, converting it to thermal energy reversibly alters the electrical capacitance[7] and therefore the excitability of nerve cells. However, direct IR stimulation is a non-specific approach that excites (or inhibits) many neurons in the area where optical illumination targets. The use of thermal energy as a stimulus to activate neurons could be highly localized to avoid generic effects on neuronal firing and their behavior. Plasmonic nanostructures such as gold nanorods (AuNRs), which serve as locoregional photothermal transducers, have been employed to modulate (inhibit/stimulate) neural activity *in vitro* using NIR light[6a, 6c, 6h, 6i, 8]. Radio-frequency magnetic-field based heating of magnetic nanoparticles has also been

demonstrated to be effective in thermal activation of ion channels and triggering action potentials in cultured neurons[9]. Magnetic nanoparticles were also used to target the motor cortex of moving mice and modulate its movement through magnetothermal stimulation[6e]. Among various nanomaterials that could transform light energy to heat, polydopamine (PDA) nanoparticles are a particularly promising candidate for neuronal modulation due to their excellent photothermal properties, biocompatibility, biodegradability, and facile surface functionalization[10]. PDA-based nanomaterials have been widely investigated as photothermal agents for photothermal cancer therapy.[10b, 11] Furthermore, due to their biocompatibility and superior interaction with cells, PDA-based nanomaterials have been shown to be promising candidates for neuronal interfacing [12].

Here, we explore the use of biocompatible and biodegradable polydopamine nanoparticles and a novel highly porous biofoam as photothermal agents to stimulate excitable cells such as neurons and cardiomyocytes with NIR light in a non-disruptive manner. This novel nanomaterial approach was utilized to localize the temperature around the excitable cells under 808 nm laser illumination. The change in the activity of neurons was monitored and quantified to understand the effect of different photothermal heating conditions. Electrical activity was measured for neurons and cardiomyocytes cultured on microelectrode array (MEA) to assess the ability of PDA nanoparticles and PDA-based foam to modulate the cell excitability. Series of quantitative analyses were performed to explain the effect of laser light intensity in the presence of PDA nanoparticles in modular and reversible control of the neuron and cardiomyocyte activity.

Results and Discussion

PDA nanoparticles are synthesized by oxidative self-polymerization of dopamine monomer in water–ethanol–ammonium mixture at room temperature, using a previously reported method [13]. Scanning electron microscopy (SEM) image and dynamic light scattering (DLS) measurement revealed the diameter of the PDA particles to be ~465 nm (Figure 1B and 1C). It has been recently reported that nanoparticle's interaction with neurons is solely dependent on its surface charge regardless of the shape, size and composition [14]. Negatively charged particles tend to adhere to the neuron cell membrane more efficiently than other particles. Polydopamine, due to the presence of hydroxyl and amine functional groups on its surface, exhibits different surface charge under different pH conditions, with an isoelectric point at 3.3 [15]. Under physiological conditions (pH=7.4), the zeta potential of PDA was measured to be −30.6 ± 0.3 mV (Figure S1). PDA particles exhibited broad optical absorption ranging from 400 nm to 800 nm with a peak around 500 nm (Figure 1D). Polydopamine nanoparticles exhibit excellent biocompatibility and biodegradability and provide high photothermal conversion efficiency and have been used as contrast agents for photothermal therapy [11a]. Although the PDA NP optical absorption is higher at lower wavelength, NIR laser (808 nm wavelength) was used for photothermal stimulation owing to the low optical absorption of soft biological tissues in the NIR region (~650–900 nm) compared to visible part of the electromagnetic spectrum [16]. NIR laser employed here confines the heat to the proximity of the photothermal nanoparticles, thus enabling locoregional neuromodulation. Under 808 nm laser irradiation (power density of 14 mW mm^{-2}), PDA particle suspension temperature increased with an increase in the concentration

of the nanoparticles. For a concentration of 400 μg ml^{-1}, the temperature increased by 25 °C within 4 minutes, although the cell experiments are not conducted for this long period to prevent cell death (Figure 1E). It is worth noting that smaller changes in temperature (± 5 °C) as would be desirable for controlling cell excitability can be achieved within a few seconds. The magnitude of temperature rise under NIR laser irradiation can be controlled by tuning the power density of the laser, which is critical to avoid photothermally-induced cell death (Figure 1F and 1G). Considering that the light absorption of cells and soft tissues in the NIR range is significantly lower compared to that in the visible part of the electromagnetic spectrum, 808 nm laser employed here confines the heat to the proximity of the photothermal nanoparticles, thus enabling locoregional neuromodulation [16].

To study the effect of nanoheating on the neuron viability, primary hippocampal neurons from prenatal rat were cultured on a substrate pre-coated with polyethylenimine (PEI) and laminin, sequentially. After 14 days *in vitro*, the neurons were immunolabeled for β-tubulin (III), which indicates good adhesion of neuron cells to the substrate and its long-term viability (Figure 2A) [6c]. The effect of photothermal heating on the viability of cultured neurons was examined by incubating them with PDA NPs and applying NIR light (Figure 2D). When irradiated with 808 nm laser at a power density of 14 mW mm^{-2} in the presence of PDA NP for 1, 2 and 5 minutes, no noticable change in the viability of the neurons compared to the control groups was observed. The viability of neurons subjected to laser with and without PDA NP remained above 90%, indicating that the photothermal stimulation can be employed to modulate neuronal activity without inducing cell death.

To investigate the effect of photothermal heating on neurons activity, hippocampal neurons were cultured on microelectrode arrays (MEAs) and extracellular activity of neurons was recorded with and without PDA treatment and NIR stimulation (Figure 2C). Neurons cultured on MEA formed a dense network of neurites around TiN recording electrodes (Figure 2B). To ensure that the activity of the cultured neurons is stable and does not change over time, extracellular activity was recorded for 30 min without PDA treatment and NIR stimulation (Figure S2). The overlaid waveform of cultured neurons exhibited stable activity without any significant change in the spike shape or amplitude over the entire recording duration (Figure 2E). Before stimulating the neurons with NIR laser in presence of PDA, the effect of PDA treatment on neurons baseline activity was examined (Figure 2F). Upon adherence of PDA nanoparticles to the plasma membrane of neurons, the mean spike rate of the neurons increased. This is possibly because the negatively charged PDA NPs induce a depolarization of the membrane potential by providing negative charge extracellularly to cause increased firing [14].

Following the formation of a complete network and reaching a stable spontaneous activity (approximately 14 days *in vitro* (DIV)), the neurons cultured on the MEAs were treated with PDA NPs (100 μg ml^{-1} final concentration) and incubated overnight. The PDA NPs adhered to neurons and the substrate and the rest of them gradually settled down and created a bed of particles on the cells and neurites which resulted in a particle-free solution before the activity recording and photothermal stimulation (Figure S3). The cross-section TEM images of the neurons incubated with PDA NP did not reveal any internalization of the nanoparticles [17]. The PDA NP-treated neurons were subjected to repeated irradiation of 808 nm laser

at different power densities for different stimulation duration (10, 20 and 30 seconds) in a back-to-back pulsatile fashion. The extracellular activity of the neurons was recorded before, during, and after the photothermal treatment (Figure 3A). It is worth noting that TiN electrodes transmit ~50% of the light at 800 nm wavelength (Figure S4). The extracellular signal recorded by each of these electrodes corresponds to a group of neurons on and around the electrodes that are irradiated by the NIR laser.

As can be noted, the neurons had spontaneous activity before any photo-stimulation. During the NIR irradiation, the number of action potentials fired reduced below spontaneous activity levels. Fewer spikes were detected for all power densities and for all durations tested (Figure 3A and 3B). The spike rate decreased monotonically with an increase in the NIR laser power density from 3 to 6 mW.mm^{-2} (Figure 3C). At laser power density of 3 mW mm^{-2}, there was only 39% reduction in the spike rate compared to before NIR stimulation. The spike rate reduction reached 98% when laser power density increased to 6 mW.mm^{-2}, suggesting an almost complete shutdown of neuron activity under these irradiation conditions. In comparison, neuron activity was recorded for cultures that were not treated with PDA NP but subjected to 808 nm laser irradiation (Figure S5). The neuron activity did not change even under a significantly higher laser power density of 14 mW mm^{-2} (Figure S5A). In the experiment without the presence of PDA particles, the mean spike rate measured before and during the laser irradiation did not change significantly. To investigate the effect of repeated laser stimulation, neuron activity was recorded for cultures treated with PDA NP and over 10 repeats of 30-second NIR pulses at 6 mW mm^{-2} where almost complete activity shutdown was observed (Figure 3D, S6). The similarity in neural spike activity observed, summarized as a correlation matrix, during different photothermal stimulation periods/cycles/pulses showed that the evoked photothermal responses were highly similar. Photothermal treatment had a culture wide and universal effect of in inhibiting neuron activity (Figure S6A). The mean spike rate for PDA NP-treated neurons was measured before the laser irradiation and after the finish of each cycle to reveal the possible permanent effect of photothermal treatment on neuron activity (Figure 3E). Although complete shutdown of extracellular activity was noted during the laser irradiation (with PDA NP and at 6 mW mm^{-2}), the mean spike rate after laser irradiation remained virtually identical to that observed before irradiation, indicating the reversible nature of the photothermal neuromodulation. Moreover, the spike shape and amplitude before and after the photothermal treatment did not show significant change for the same experiment indicating that neurons recovered their activity after photothermal treatment with no sign of temporary or permanent damage (Figure S7).

Following the NIR irradiation period that resulted in complete inhibition of the neural activity, we noted that the neurons do not start firing immediately after stopping the irradiation but recovered their baseline activity after a short time lag. We investigated the dependence of the neural activity recovery time on the laser power density and laser irradiation duration (Figure 4). By fixing the irradiation duration and increasing the laser power density from 3 to 6 mW mm^{-2}, the activity recovery time (the period between the end of NIR irradiation and the first spike for each electrode) increased significantly for all of the laser durations tested (Figure 4A). There was a small increase in the recovery time with an increase in the laser power density from 3 to 4 mW mm^{-2}. An increase in the laser power density from 4 to 6 mW mm^{-2}, resulted in a much larger increase in the lag time

(Figure 4C). This is possibly due to the long cooling period required at higher laser power densities, where the maximum temperature under laser irradiation is higher (Figure 1F). Alternately, stronger hyperpolarization during photo-stimulation period that at higher laser power densities could also result in longer recovery of resting membrane potential which could underlie similar monotonic increase in recovery time with response strength. In the case of fixed laser power density, an increase in the laser irradiation duration resulted in a monotonic increase in the activity lag time (Figure 4B). This increase in the activity lag time was more pronounced at the higher laser power density of 6 mW mm^{-2} (Figure 4D). The particles on the substrate immediately adjacent to the neurons also contribute to the localized heating and delay the cooling process once the laser is turned off, thus causing a significant lag in the neuron activity recovery after each photothermal stimulation cycle. The tunable activity lag time with the laser power density and laser irradiation duration serves as an additional handle in light-based neuromodulation. On the other hand, specific targeting of the photothermal nanostructures to the neurons can minimize the non-specific adsorption of the nanostructures on the substrate and possibly minimize the activity lag time.

To test the generality of photothermal modulation on controlling cellular excitability, we have investigated the effect of PDA NPs and laser treatment on the electrical activity of cardiomyocytes. The iPSC-derived cardiomyocytes were differentiated and plated on the MEAs to assess the beating rates of cardiac tissues (Figure 5A). Without PDA NPs, upon laser stimulation, the beating rates of cardiac tissues increased only slightly (less than 10%) and recovered to baseline rate once the laser irradiation is stopped (Figure 5B and 5C). Following the incubation of cardiomyocytes with PDA nanoparticles for 24 hours, the beating rates under laser irradiation increased significantly compared to untreated cells subjected to laser irradiation (Figure 5D and 5E and supporting information Figure S8). These results indicate the successful modulation of the electrical activity of the cardiomyocytes with photothermal nanostructures. To further understand the effect of localized heating on the tissue, PDA NP-treated tissues were subjected to different laser power densities from 4 to 25 mW mm^{-2} (Figure 5F–H and supporting information Figure S9). With an increase in the laser power density from 4 to 14 mW mm^{-2}, the beating rate progressively increased and reached to about 1.8 times of the baseline activity (Figure 5F). For the highest laser power density (25 mW mm^{-2}), the cardiomyocytes exhibited irreversible changes in the beating rate, indicating possible thermal toxicity (Figure S9). The tissues not treated with PDA NPs exhibited only a small increase in the beating rate with a maximum increase of less than 10% at 14 mW.mm^{-2}. These results demonstrate that the iPS-derived cardiac tissues showed a significant response to the localized nano-heating in the presence of PDA NPs with NIR laser irradiation. Also, the nature of the response changed from excitatory at lower laser power densities to inhibitory at laser power densities above 14 mW mm^{-2} (Figure 5 and S9). The tunable modulation of the electrical activity of cardiomyocytes using PDA NPs could be harnessed for excitation and inhibition of cardiac activity is desired, simply by changing the laser power density.

The results discussed so far involve the incubation of the neurons (or cardiomyocytes) with colloidal PDA NP, which offers poor control over the distribution of the photothermally-active nanostructures. To achieve better spatial control over photothermal stimulation and better photothermal performance, we have designed a highly porous 3D collagen foam

modified with PDA NPs as a conformal photothermal substrate (Figure 6A). Collagen foam is widely used in biomedical applications (e.g., wound dressing, tissue culture scaffolds) due to its highly porous structure and excellent biocompatibility.[18] Pristine collagen foam is white (due to light scattering) and does not possess photothermal activity (Figure S10A). When the collagen foam is exposed to a high concentration solution of PDA nanoparticles, within a few minutes, the collagen fibers are completely covered with PDA nanoparticles, as is indicated by its change of color from white to black (Figure S10B). SEM images of the PDA-modified collagen foam (PDA/Collagen) reveal the high porosity and the PDA nanoparticles adsorbed on individual collagen fibers (Figure 6B). The PDA/collagen foam was found to be highly stable with no noticeable desorption of the PDA NP even under mechanical agitation. The absorbance spectrum of the PDA/collagen foam is similar to that of PDA NP solution suggesting that photothermal efficiency for the foam should be similar to the PDA NPs (Figure 6C). In its dry state, the surface temperature of PDA/collagen foam increased by more than 100 °C in just less than 10 seconds when irradiated by laser at a power density of 6 mW mm^{-2} (Figure S11). Even at a much lower laser power density of 3 $mW.mm^{-2}$, we noted a 60 °C increase in the local surface temperature within the first 10 seconds. In wet state, the foam surface temperature rose by up to 12 °C after 10 seconds and by up to 20 °C after 30 seconds of irradiation at a laser power density of 6 mW mm^{-2} (Figure 6D). The superior photothermal activity of the PDA/collagen foam compared to the high concentration of PDA NPs (100 μg ml^{-1}) stems from the highly dense adsorption of the PDA NPs on the collagen fibers and efficient light trapping within the foam due multiple reflections. In addition to the excellent photothermal properties, the highly porous PDA/collagen foam soaked in the cell culture medium can be applied as a conformal patch on cells and tissues.

To investigate the efficacy of PDA/collagen foam in photothermally modulating the neural activity, the foam was placed on the neurons cultured on the MEAs for 14 DIV, and after the neurons reached stable spontaneous activity. The neurons with PDA/collagen foam were subjected to repeated irradiation of 808 nm laser at different power densities for different stimulation durations (10, 20 and 30 seconds). The extracellular activity of the neurons was recorded during the photothermal treatment and it is evident that spiking activity during the photothermal stimulation is reduced drastically (Figure 6E and 6F). The quantitative measurement of the changes in the spike rate showed that at all the power densities tested, the neuron activity suppression was above 90% (Figure 6G). In comparison, at the same power density of 3 mW mm^{-2}, photothermal treatment of neurons treated with colloidal PDA NP resulted in only a 39% reduction in neuron activity. Moreover, when the power density was increased to 15 $mW.mm^{-2}$, PDA/collagen foam resulted in permanent damage to cells, and the activity suppression was not reversible. This superior photothermal performance of the PDA/collagen compared to colloidal PDA NP allows the utilization of lower power light sources (e.g. near-infrared LEDs) instead of laser for modulating the neural activity. Furthermore, this PDA/collagen 3D foam could be easily applied as a patch on brain tissues and cardiac tissues for modulating the electrical activity in a facile manner.

Conclusions

In conclusion, we have demonstrated the reversible and graded control of the electrical activity of excitable cells using PDA nanoparticles as biocompatible and biodegradable photothermal transducers. In the presence of PDA nanoparticles, the spike rate of neurons was significantly suppressed under NIR laser irradiation with a power density as low as 3 mW mm^{-2}. With a progressive increase in the laser power density, we observed a monotonic decrease in the spike rate. The activity recovery time was found to be dependent on irradiation power density and irradiation duration. The neural activity suppression and recovery were repeatable over 10 consecutive pulses of laser irradiation in a single trial, demonstrating the robustness of this non-invasive neuromodulation approach. In the presence of PDA nanoparticles, the beating rate of cardiomyocyte tissues progressively increased as the irradiation laser power density increased from 4 to 14 mW mm^{-2}. To improve the ease of interfacing the photothermal agents with neural cultures and brain tissues, we have designed and realized a 3D collagen/polydopamine nanoparticle foam and applied it on the cultured neurons as an “add-on” patch. The 3D foam demonstrated superior photothermal and neuromodulation performance compared to colloidal polydopamine nanoparticles in that we observed more than 90 percent reduction in neuron activity even at laser power densities as low as 3 mW mm^{-2}. Compared to inorganic photothermal nanostructures (e.g., noble metal nanoparticles), PDA nanostructures are better suited for *in vivo* neuromodulation owing to their high biocompatibility and biodegradability. We believe that this novel material platform for non-invasive neuromodulation can be easily extended to other excitable cells both *ex vivo* and *in vivo* and serve as a valuable tool in nano-neuroengineering.

Experimental Section

Cell Culture:

All procedures have been approved by the Institutional Animal Care and Use Committee (IACUC) at Washington University in St. Louis. Hippocampal tissues were dissected from embryonic day 18 Sprague Dawley rat brain (Charles River, USA). The tissues were transferred into Hibernate EB medium (HEB, BrainBits, USA) for further use. Cell dissociation solution was prepared by dissolving 6 mg papain (P4762, Sigma, USA) in 3 ml of Hibernate E-Ca (HE-Ca, BrainBits, USA). Hippocampal tissues were transferred to the cell dissociation solution and incubated at 30 °C for 10 minutes. Dissociation solution was removed and HEB medium was added to the tissues, followed by trituration with fire-polished Pasteur pipette. Cell dispersion was centrifuged (200×g, 1 minute) and supernatant was removed, and pellets were resuspended in NbActiv4 (BrainBits, USA). Substrates were pre-treated with poly(ethyleneimine) solution (0.1 % in water, P3143, Sigma, USA) for 30 minutes followed by air drying. Before the cell seeding, substrates were treated with laminin solution (20 μg ml^{-1} in NbActiv4 medium, L2020, Sigma, USA). After removing the extra laminin solution, cells were seeded at the density of 500–1000 cells.mm^{-2} and maintained in the NbActiv4 medium in a humidified incubator with 5% CO_2 and 37 °C condition. After 2 days, half of the medium was changed with fresh NbActiv4 medium and was regularly changed every 4 days.

For iPS-derived cardiomyocytes (iPS-CMs), the WTC-11-GCaMP6 from Bruce Conklin Lab in Gladstone Institute were used as the induced pluripotent stem cells (iPSC). The iPSCs were maintained in E8 medium (Thermo Fisher Scientific) on Matrigel-coated (Corning) tissue culture plate and passaged every four days. The protocols used to differentiate and purify iPS-derived cardiomyocytes (iPS-CMs) was through Wnt modulation and lactate purification that was previously described [19].

Polydopamine Nanoparticle and Collagen/Polydopamine Foam Preparation:

All chemicals were purchased from Millipore Sigma, St. Louis, USA and used without further modification. Polydopamine particles were synthesized by using a method described elsewhere.[13] In a typical synthesis procedure of polydopamine nanoparticles, 252 mL of deionized (DI) water (resistivity >18.2 MΩ·cm) was mixed with 112 mL of ethanol in a 1000 mL glass container. Subsequently, 1.96 mL of aqueous solution of ammonia (28–30% NH4OH) was introduced into the above water/ethanol mixture. After stirring for 30 min, the aqueous solution of dopamine hydrochloride (1.4 g in 28 mL) was added to the above solution. The reaction was left under gentle magnetic stirring for 24 h with no cap on the glass container. The PDA particles were collected by centrifugation (9000 rpm, 10 min) and washed with DI water three times and dispersed in water (320 mL).

To prepare the photothermally active 3D foam, a collagen film (HeliTAPE Collagen Wound Dressing, Miltex® Instruments, USA) was soaked in water to create a hydrogel. The collagen hydrogel wass then freeze-dried to achieve a highly porous 3D foam. The collagen foam, was soaked in the PDA NP solution (1 mg ml^{-1} in water) and left for 5 minutes with shaking followed by washing with water to remove the excess nanoparticles. The PDA NP-loaded collagen foam was freeze-dried again to be used in the photothermal stimulation experiments.

Material Characterization: Scanning electron microscopy (SEM) images were obtained by using a JEOL JSM-7001 LVF Field Emission scanning electron microscope. Dynamic light scattering (DLS) and zeta potential measurements were performed using Malvern Zetasizer (Nano ZS). Shimadzu UV-1800 spectrophotometer was employed for light absorption measurements.

Photothermal Stimulation:

A fiber optic NIR laser (808 nm) was used for a light source and the laser beam spot size and power density was controlled by its distance from the microelectrode array (MEA, Multichannel Systems, Germany). Hippocampal neuronal networks were cultured on a MEA chip and incubated with PDA NPs overnight. The PDA NP-treated neurons were then repeatedly irradiated with a NIR laser (808 nm) at different power densities and durations. A typical photothermal experiment lasts for 330 seconds, and the cells were illuminated with laser at different power densities for 10, 20 and 30 seconds. The laser on and off was controlled by a mechanical shutter. For repeatability experiment, cells were illuminated for 30 seconds with a power density of 6 mW mm^{-2} followed by 90 seconds of no laser illumination for 10 cycles. The experiment for calculating the neuron activity recovery time after laser illumination was performed by recording the activity for 60 seconds followed by

laser pulses with different durations and power densities followed by at least 90 seconds wait time, for a total of 210 seconds. Same experimental procedures were followed for cardiomyocytes.

Electrical Activity Recording:

Neural recordings were obtained from neuronal cultures at the age of 14–18 DIV. Extracellular activity from cultured neurons were monitored using 60-channel TiN microelectrode arrays (MultiChannel Systems, diameter 30 μm, electrode spacing 200 μm, 500 nm thickness of Si3N4 insulator). Electrode signals were amplified and digitized with an *in vitro* MEA system (Multichannel systems, gain 1100, bandwidth 10–8 kHz, sampling frequency 25 kHz). The recorded signals were filtered with a 200 Hz digital high pass filter (Butterworth, second order), and spikes were detected by setting the threshold level at five times the standard deviation of background noise using vendor provided software (MC Rack, MultiChannel Systems). Recording condition was maintained at 37 °C and 5% CO_2. Collected data were processed using MATLAB (MathWorks). For bulk heating experiments, the head stage temperature was adjusted to desired value and after 15 minutes of stabilization, the neuron activity recording was performed. To test the effect of PDA NP on neuron activity without laser stimulation, the extracellular activity of cultured neurons was recorded for 30 minutes before addition of PDA NP after which the culture was incubated with PDA NP solution (100 μg ml^{-1} final concentration).

To record the field potential activities of iPS-CM, the iPS-CMs were suspended at 30×10^6 cells ml^{-1} and a 4 μl droplet was seeded on the recording area of MEA probe (60MEA200/10iR-Ti). The field potentials were recorded using MC_Rack software (Multichannel Systems) at 10000 Hz sampling rate with a 200 Hz digital high pass filter (Butterworth, second order). The data were converted to ABF format using MC_Data Tool (Multichannel Systems) and the field potentials were analyzed using Clampfit 10.7 (Molecular Devices) and MATLAB (MathWorks).

Cell Viability: Hippocampal neurons were cultured in pre-treated 96 well black plates at the density of 20000 cells per well for 14 DIV and treated with PDA NPs at 100 μg ml^{-1} final concentration. After 5 h incubation, they were subjected to 808 nm laser for 10 minutes at a power density of 14 mW mm^{-2}. After 24 hours, MTS assay was performed as per manufacturer protocol.

Data Analysis:

Recording channels whose average firing rate was larger than 0.1 spikes per second were selected as active channels and used for neural activity analysis. For the analysis of spontaneous activity, peri-event time histogram and raster plots were used with the NIR irradiation as an event. The spike rate reduction (ΔR/R) with or without the NIR irradiation was calculated by the following equation: $\Delta R/R\ (\%) = [R(ON) - R(OFF)]/R(OFF)$, where R(OFF) and R(ON) indicated the average spike rate before and after the onset of NIR irradiation, respectively. R(ON) covered the entire irradiation period (5–45 seconds), and R(OFF) covered the 30 second window just before the onset of the irradiation. All statistics were performed with 5% one-sided significance level.

Immunostaining: Hippocampal neurons were fixed in 4% neutral buffered formalin in 1x PBS for 30 minutes at room temperature and washed with PBS three times. To permeabilize the cells, neurons were incubated with 0.5% Triton X-100 in 1x PBS for 10 minutes at room temperature and washed with PBS three times. The nonspecific binding of antibodies was blocked by 6% bovine serum albumin (BSA, Sigma) in PBS for 30 minutes, and washed with PBS once. The biotinylated primary antibody (neuron-specific β-III tubulin antibody, 6 μg ml^{-1} in 1.5% BSA, R&D systems MAB 1195) was added to the cells and incubated for 3 h at RT. After washing with PBS for three times, streptavidin-tagged fluorescent dye (IRDye 800CW Streptavidin, 50 ng ml^{-1} in 1.5% BSA, LI-COR) were incubated with the cells for 30 minutes at RT. After washing with PBS for three times, DAPI solution (300 nM in PBS, Sigma) was used for nucleus staining. Fluorescence images were obtained using Lionheart FX Automated Microscope (BioTek, USA). The iPSC-derived cardiomyocytes were seeded on glass slide at Day 30. The cells were fixed with 4% (v/v) paraformaldehyde for one hour and stained with primary antibody TNNT2 (ab45923; Abcam) and secondary antibody Alexa Fluor 488 goat anti-rabbit IgG (A11008; Invitrogen) and nuclei counterstained by DAPI solution (1 μg mL^{-1}).

Supplementary Material

Refer to Web version on PubMed Central for supplementary material.

Acknowledgements

The authors acknowledge support from Air Force Office of Scientific Research (#FA95501910394 (SS and BR)) and National Institutes of Health (R01-HL136553 (JRS)). The authors thank Nano Research Facility (NRF) and Institute of Materials Science and Engineering at Washington University for providing access to electron microscopy facilities.

References

[1]. a) Won SM, Song E, Zhao J, Li J, Rivnay J, Rogers JA, Advanced Materials 2018, 30, 1800534;b)Li J, Duan H, Pu K, Advanced Materials2019, 31, 1901607;c)Fattahi P, Yang G, Kim G, Abidian MR, Advanced materials2014, 26, 1846; [PubMed: 24677434] d)Jeong YC, Lee HE, Shin A, Kim DG, Lee KJ, Kim D, Advanced Materials2020, 1907522;e)Obidin N, Tasnim F, Dagdeviren C, Advanced Materials2020, 32, 1901482.

[2]. Li J, Pu K, Chemical Society Reviews2019, 48, 38. [PubMed: 30387803]

[3]. a)Boyden ES, Zhang F, Bamberg E, Nagel G, Deisseroth K, Nature Neuroscience2005, 8, 1263; [PubMed: 16116447] b)Zemelman BV, Lee GA, Ng M, Miesenböck G, Neuron2002, 33, 15. [PubMed: 11779476]

[4]. a)Bernstein JG, Boyden ES, Trends in Cognitive Sciences2011, 15, 592; [PubMed: 22055387] b)Deisseroth K, Feng G, Majewska AK, Miesenböck G, Ting A, Schnitzer MJ, Journal of Neuroscience2006, 26, 10380; [PubMed: 17035522] c)Callaway EM, Yuste R, Current opinion in neurobiology2002, 12, 587. [PubMed: 12367640]

[5]. Wang Y, Guo L, Frontiers in Neuroscience2016, 10, 69. [PubMed: 27013938]

[6]. a)Yoo S, Park J-H, Nam Y, ACS nano2018, 13, 544;b)Rastogi SK, Garg R, Scopelliti MG, Pinto BI, Hartung JE, Kim S, Murphey CGE, Johnson N, San Roman D, Bezanilla F, Cahoon JF, Gold MS, Chamanzar M, Cohen-Karni T, Proceedings of the National Academy of Sciences2020, 117, 13339;c) Yoo S, Hong S, Choi Y, Park J-H, Nam Y, ACS Nano 2014, 8, 8040; [PubMed: 25046316] d)Carvalho-de-Souza João L., Treger Jeremy S., Dang B, Kent Stephen B. H., Pepperberg David R., Bezanilla F, Neuron2015, 86, 207; [PubMed: 25772189] e)Munshi R, Qadri SM, Zhang Q, Rubio IC, Del Pino P, Pralle A, Elife2017, 6, e27069; [PubMed: 28826470]

f)Kang H, Lee G-H, Jung H, Lee JW, Nam Y, ACS Nano2018, 12, 1128; [PubMed: 29402086] g)Lee JW, Jung H, Cho HH, Lee JH, Nam Y, Biomaterials2018, 153, 59; [PubMed: 29102745] h)Eom K, Kim J, Choi JM, Kang T, Chang JW, Byun KM, Jun SB, Kim SJ, Small2014, 10, 3853; [PubMed: 24975778] i)Yoo S, Kim R, Park J-H, Nam Y, ACS Nano2016, 10, 4274. [PubMed: 26960013]

[7]. Shapiro Mikhail G., Homma Kazuaki, Villarreal Sebastian, Richter C-P, Bezanilla F, Nature Communications2012, 3, 736.

[8]. Yong J, Needham K, Brown WGA, Nayagam BA, McArthur SL, Yu A, Stoddart PR, Advanced Healthcare Materials2014, DOI: 10.1002/adhm.201400027n/a.

[9]. a)Dobson J, Nat Nanotechnol2008, 3, 139; [PubMed: 18654485] b)Huang H, Delikanli S, Zeng H, Ferkey DM, Pralle A, Nat Nanotechnol2010, 5, 602. [PubMed: 20581833]

[10]. a)Batul R, Tamanna T, Khaliq A, Yu A, Biomaterials science2017, 5, 1204; [PubMed: 28594019] b)Seth A, Gholami Derami H, Gupta P, Wang Z, Rathi P, Gupta R, Cao T, Morrissey JJ, Singamaneni S, ACS applied materials & interfaces2020, 12, 42499. [PubMed: 32838525]

[11]. a)Liu Y, Ai K, Liu J, Deng M, He Y, Lu L, Advanced Materials2013, 25, 1353; [PubMed: 23280690] b)Zhang D-Y, Zheng Y, Zhang H, Sun J-H, Tan C-P, He L, Zhang W, Ji L-N, Mao Z-W, Advanced Science2018, 5, 1800581. [PubMed: 30356964]

[12]. a)Kang K, Lee S, Kim R, Choi IS, Nam Y, Angewandte Chemie2012, 124, 13278;b)Battaglini M, Marino A, Carmignani A, Tapeinos C, Cauda V, Ancona A, Garino N, Vighetto V, La Rosa G, Sinibaldi E, ACS Applied Materials & Interfaces2020, 12, 35782; [PubMed: 32693584] c)Golabchi A, Wu B, Cao B, Bettinger CJ, Cui XT, Biomaterials2019, 225, 119519. [PubMed: 31600673]

[13]. Ai K, Liu Y, Ruan C, Lu L, Lu G, Advanced Materials2013, 25, 998. [PubMed: 23239109]

[14]. Dante S, Petrelli A, Petrini EM, Marotta R, Maccione A, Alabastri A, Quarta A, De Donato F, Ravasenga T, Sathya A, Cingolani R, Proietti Zaccaria R, Berdondini L, Barberis A, Pellegrino T, ACS Nano2017, 11, 6630. [PubMed: 28595006]

[15]. Gholami Derami H, Jiang Q, Ghim D, Cao S, Chandar YJ, Morrissey JJ, Jun Y-S, Singamaneni S, ACS Applied Nano Materials2019, 2, 1092.

[16]. a)Weissleder R, Nature Biotechnology2001, 19, 316;b)Smith AM, Mancini MC, Nie S, Nature Nanotechnology2009, 4, 710.

[17]. a)Jo DH, Kim JH, Lee TG, Kim JH, Nanomedicine: Nanotechnology, Biology and Medicine2015, 11, 1603;b)Wong Y, Markham K, Xu ZP, Chen M, Lu GQ, Bartlett PF, Cooper HM, Biomaterials2010, 31, 8770. [PubMed: 20709387]

[18]. a)Aslan B, Guler S, Tevlek A, Aydin HM, Journal of Biomedical Materials Research Part B: Applied Biomaterials2018, 106, 2157; [PubMed: 29024376] b)Mackenzie SJ, Yi JL, Singla A, Russell TM, Osterhout DJ, Calancie B, Muscle & Nerve2018, 57, E78. [PubMed: 28746726]

[19]. a)Lian X, Hsiao C, Wilson G, Zhu K, Hazeltine LB, Azarin SM, Raval KK, Zhang J, Kamp TJ, Palecek SP, Proc. Natl. Acad. Sci. USA2012, 109, E1848; [PubMed: 22645348] b)Tohyama S, Hattori F, Sano M, Hishiki T, Nagahata Y, Matsuura T, Hashimoto H, Suzuki T, Yamashita H, Satoh Y, Cell stem cell2013, 12, 127. [PubMed: 23168164]

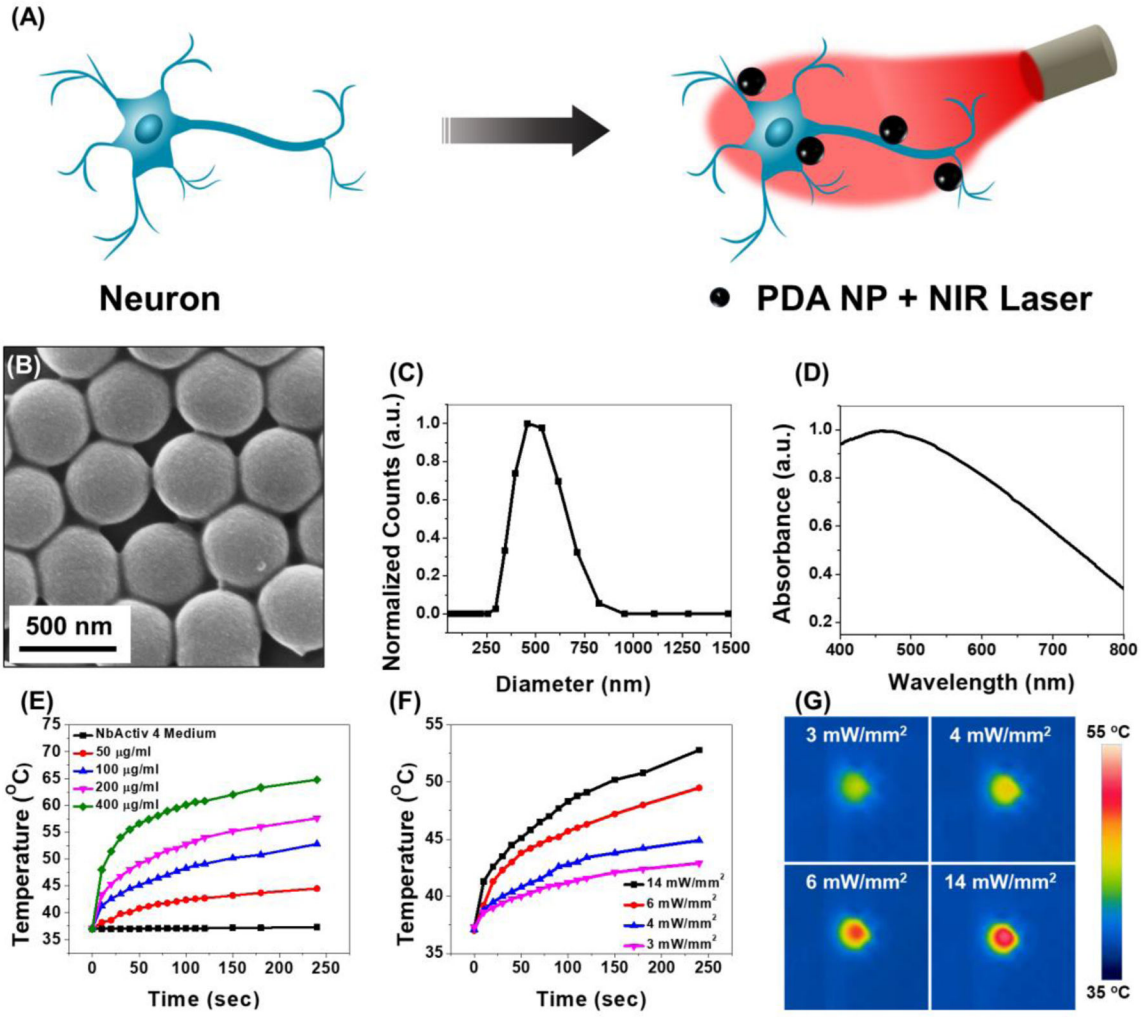

Figure 1.

(A) Schematic of polydopamine nanoparticle (PDA NP)-mediated photothermal stimulation of neurons. PDA nanoparticles localized on the neuron membrane, modulates the neural activity through photothermal conversion of NIR light. (B) SEM image, (C) DLS measurement and (D) Absorption spectra of PDA NPs. (E) Temperature changes in PDA NP solution with different concentrations at 14 mW mm^{-2} laser power density. (F) Temperature changes in 100 µg ml^{-1} solution of PDA NP at different laser power density and (G) Corresponding IR camera images of the PDA NP solution at the end of the laser illumination period.

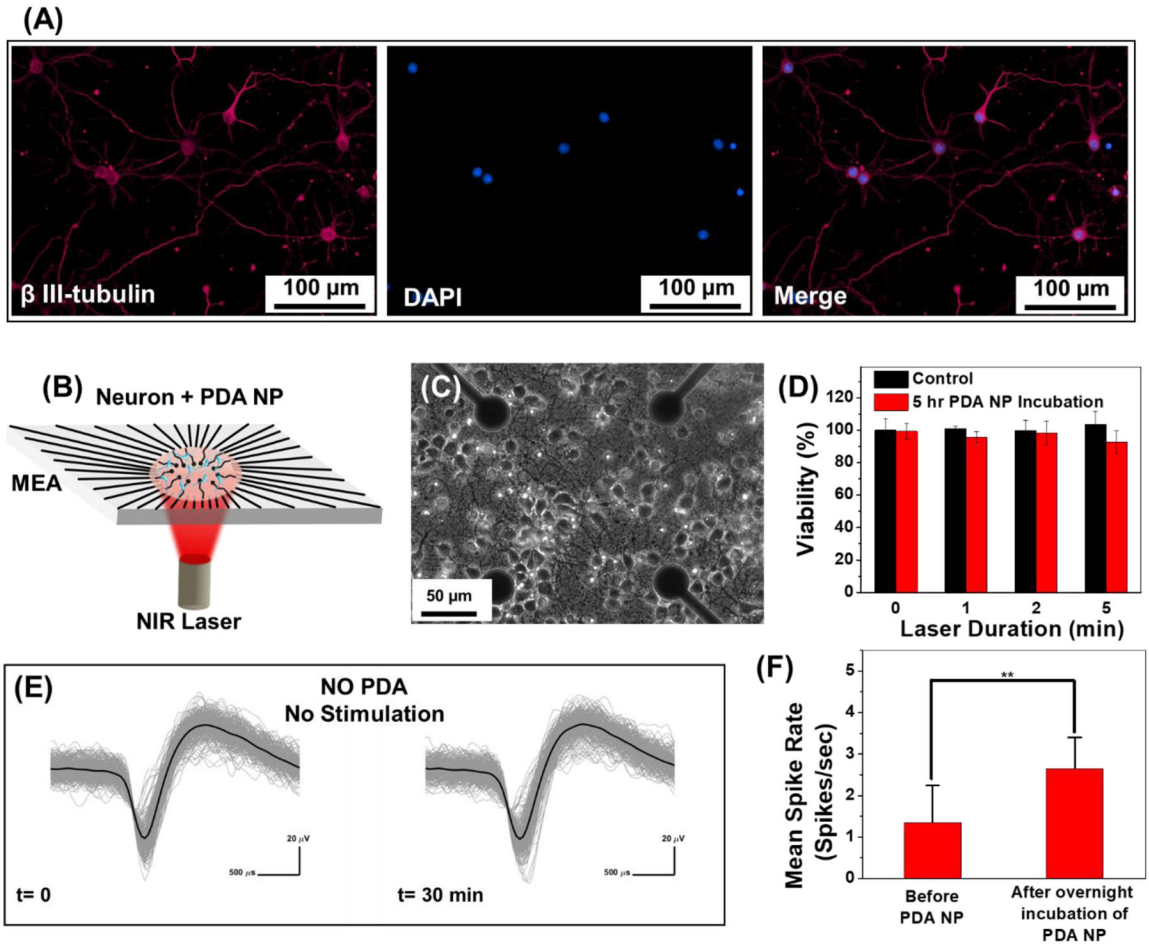

Figure 2.

(A) Fluorescence images of cultured hippocampal neurons after immunochemical staining with β-tubulin (III) (magenta) and nucleus (blue). (B) Schematic of the experimental setup with neurons cultured on a microelectrode array (MEA) and stimulated with NIR laser with and without PDA NP treatment. (C) Phase contrast image of the hippocampal neurons cultured on PEI-laminin coated MEA with cell density of 1000 cells mm^{-2}. (D) Cell viability of neurons subjected to 1, 2 and 5 minutes of NIR irradiation (14 mW mm^{-2}) without PDA NP (control) and with PDA NP (100 μg ml^{-1} final concentration). The heat generated by NIR laser in presence of PDA NP did not change the viability of the neurons compared to control sample (no PDA NP), meaning that it is safe to use PDA NP for photothermal treatment of neurons. (E) Overlaid waveform of hippocampal neurons at half an hour time interval. Neurons were not treated with PDA NP and are not subject to any external stimulation. Spikes from 3-minute recording with 256 spikes in each set (no change in mean spike rate). Black curve shows the mean value for each set. (F) Effect of localization of PDA NP on neuron membrane on the mean spike rate of cultured neurons without NIR stimulation. Unpaired Two-samples t-test; p= 0.0015, n=21, * p<0.05, ** p<0.01, *** p<0.001 and **** p<0.0001.

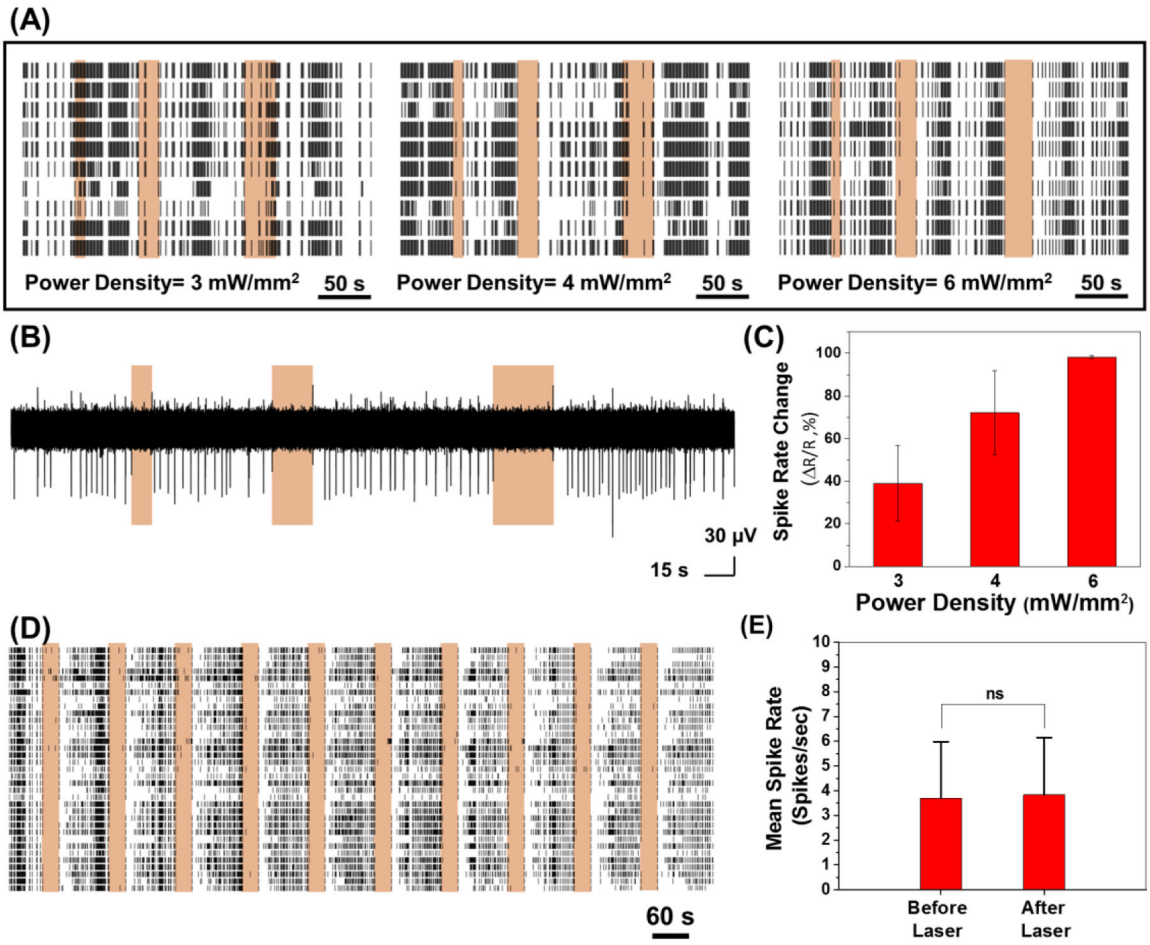

Figure 3.

(A) Spike rates of neurons treated with PDA NP (100 μg ml^{-1}) with NIR irradiation at different power densities. (B) A single trace of spike recording for different NIR irradiation periods (10 s, 20 s and 30 s laser irradiation at power density of 6 mW mm^{-2}). (C) Quantification of spike rate changes in panel A (effect of laser power density on spike rate change and inhibition of neuron activity). (D) Spike rates of neurons treated with PDA NP (100 μg ml^{-1}) with NIR irradiation (power density of 6 mW mm^{-2}) over 10 cycles of 30 s treatment. (E) Mean spike rates of PDA NP-treated neurons before and after NIR irradiation (Data were collected for laser power density of 6 mW mm^{-2} where neuron activities were completely suppressed during NIR irradiation, Unpaired Two-samples t-test; p= 0.8866, n=55).

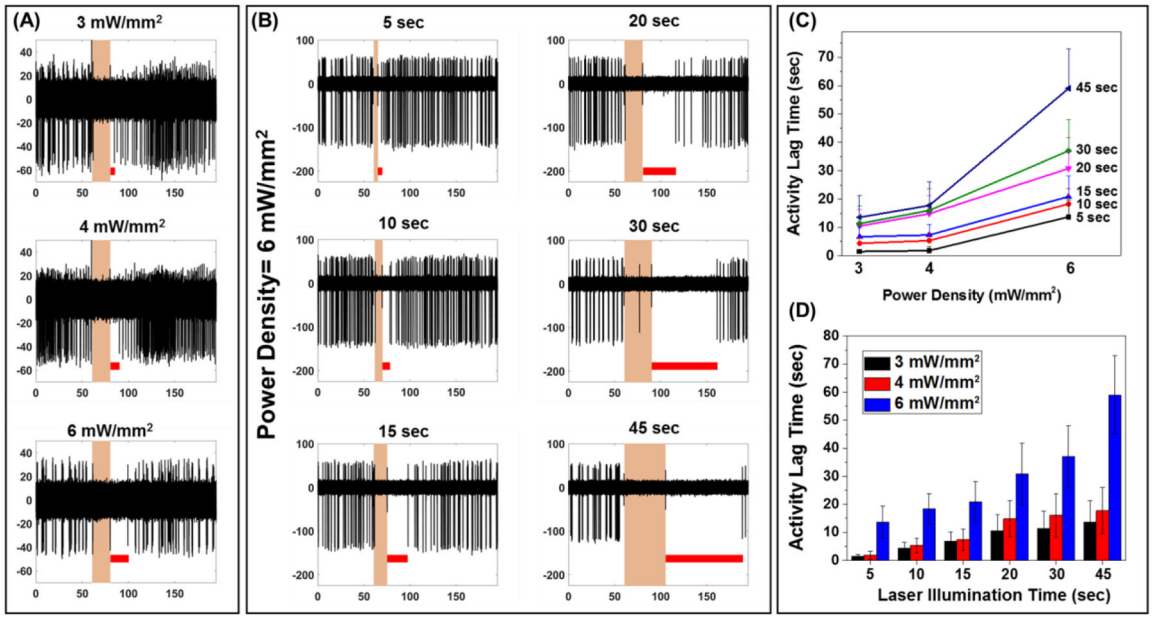

Figure 4.

(A) A single trace of spike recording for neurons treated with PDA NP at different laser power densities for 20 s. Red lines show the activity lag time which is the amount of time it took after the laser illumination for the first spike to appear. (B) Effect of laser duration on the activity lag time for PDA NP treated neurons (power density of 6 mW mm^{-2}). (C) Quantification of the effect of the laser duration on the activity lag time at different laser power densities. (D) Quantification of the effect of the laser power density on the activity lag time at different laser duration times.

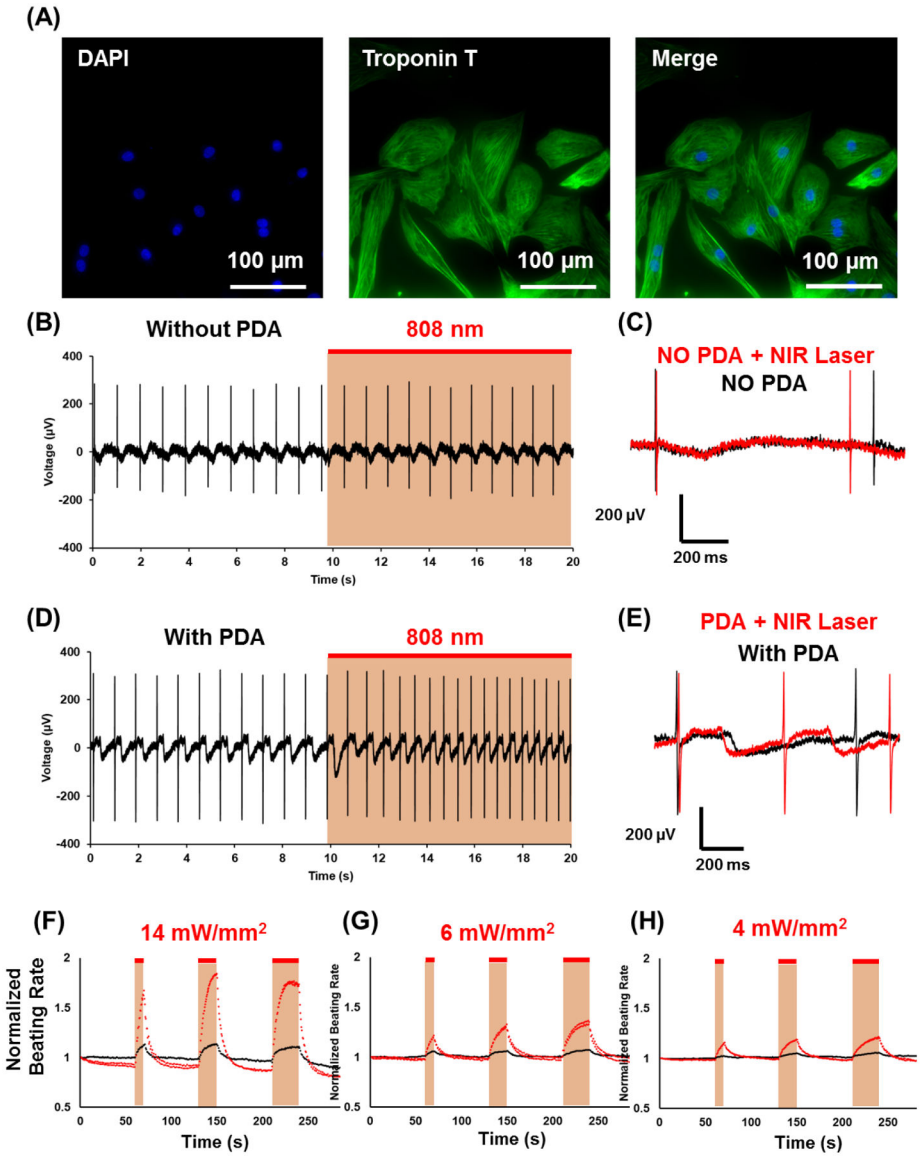

Figure 5.

(A) The immunofluorescence images of iPSC-derived cardiomyocyte counter stained with DAPI (blue) and cardiac troponin T (green). PDA nano-particles increased the beating rates of iPS-derived cardiomyocytes. (B) The original trace of field potential recording of iPS-derived cardiomyocytes from MEA system without PDA treatment. The laser power density was 14 mW.mm^{-2} and was turned on for 10 seconds as indicated. (C) The representative traces of field potential recordings of iPS-CMs without treating with PDA nanoparticles before (black) and after (red) 808 nm laser excitation. (D) The original trace of field potential recording of iPS-derived cardiomyocytes from MEA system. The iPS-CMs were treated with PDA nanoparticles for 24 hrs and washed out before recording. The laser power density was 14 mW mm^{-2} and was turned on for 10 seconds as indicated. (E) The representative traces of field potential recordings of iPS-CMs treated with PDA nanoparticles before (black) and after (red) 808 nm laser excitation. (F) – (H) The

normalized beating rates of iPS-CMs before and after 808 nm laser excitation. At different laser power densities (14, 6 and 4 mW mm^{-2}), the laser was turned on for 10, 20 and 30 seconds at the indicated time (the red lines show the data for experiments with PDA and laser, and black lines show data for only laser irradiation). The beating rates were determined by calculating the peak intervals of field potential recordings and normalized the rates at baseline.

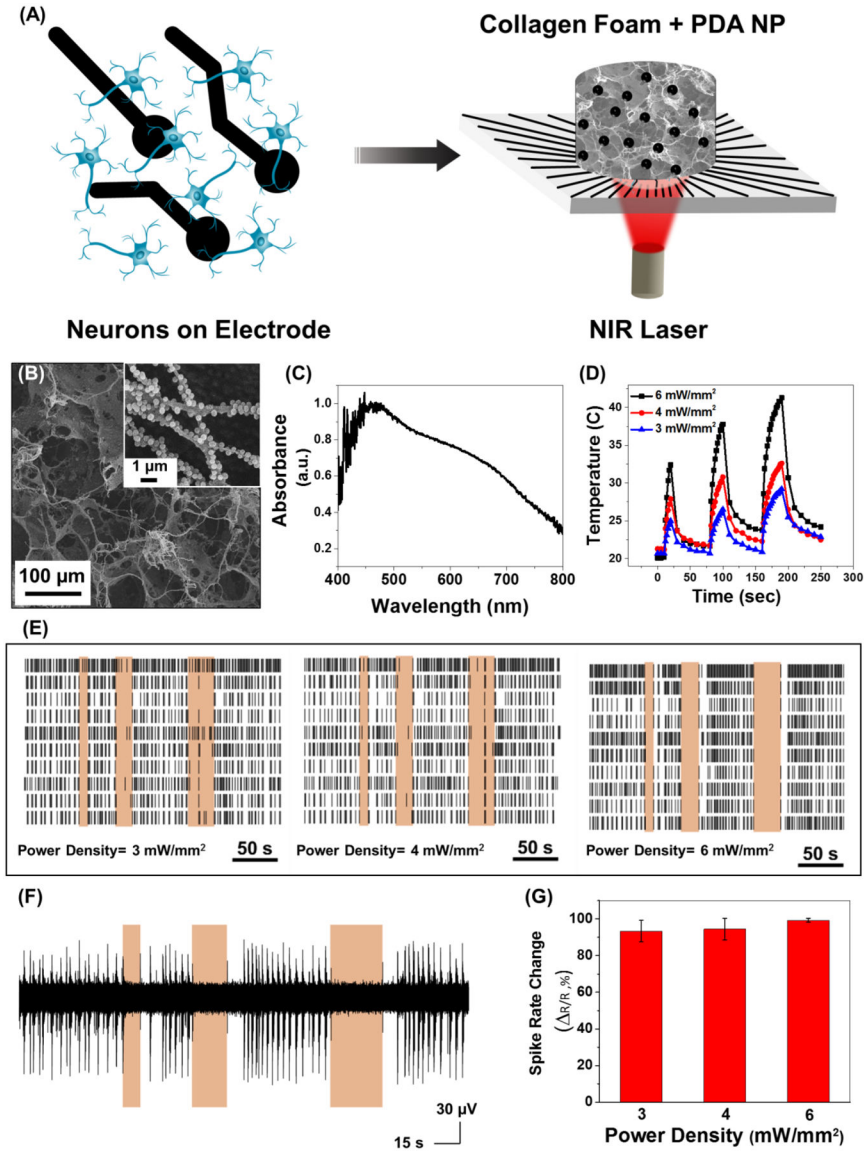

Figure 6.

(A) Schematic of experimental setup with neurons cultured on a microelectrode array (MEA), collagen foam loaded with PDA NP placed on the culture and stimulated with NIR laser. (B) SEM image (inset: higher magnification SEM) and (C) Absorption spectra of collagen foam loaded with PDA NP. (D) Temperature changes of collagen foam + PDA NP in wet state at different laser power densities. (E) Spike rates of neurons with collagen foam loaded with PDA NP and NIR irradiation at different power densities. (F) A single trace of spike recording for different NIR irradiation periods (10 s, 20 s and 30 s laser irradiation at power density of 6 mW mm^{-2}). (G) Quantification of spike rate changes in panel E (effect of laser power density on spike rate change and inhibition of neuron activity).